Picosecond electron-hole droplet formation in indirect-gap $Al_xGa_{1-x}As$

H. Kalt, K. Reimann, W. W. Rühle, M. Rinker, and E. Bauser
Max-Planck-Institut für Festkörperforschung, Heisenbergstrasse 1, D-7000 Stuttgart 80, Federal Republic of Germany
(Received 10 April 1990)

A phase separation into a liquid and an exciton gas is found for the optically generated electron-hole system in indirect-gap $Al_xGa_{1-x}As$. The formation of electron-hole droplets occurs on a time scale of a few hundred picoseconds, i.e., much more rapidly than in Si or Ge. This rapid droplet formation is found in $Al_xGa_{1-x}As$ regardless of whether it is an indirect-gap semiconductor due to its alloy composition or due to application of hydrostatic pressure. A subnanosecond phase separation is, however, not observed in GaAs, which is an indirect-gap semiconductor under hydrostatic pressure. This gives strong evidence that the accelerated nucleation dynamics is caused by alloy disorder. We determine the equilibrium density and critical temperature of the liquid phase from a preliminary phase diagram to be 4.5×10^{18} cm^{-3} and 34 K, respectively. The electron-hole plasma with density and temperature above the critical parameters is still bound with respect to the free exciton and shows self-confinement.

I. INTRODUCTION

The condensation of an electron-hole system into a liquid state in equilibrium with an excitonic gas is well established in the indirect-gap semiconductors Si and Ge.[1,2] Growth of electron-hole droplets up to macroscopic size is observed as a consequence of extremely long carrier lifetimes in these materials.[3] In contrast, carrier lifetimes are too short to allow an equilibrium phase separation in direct-gap semiconductors such as GaAs or CdS.[4,5] Experimental results are consistently described here by a nonequilibrium dynamics of small electron-hole clusters.[4]

The semiconductor alloy $Al_xGa_{1-x}As$ represents in this context an intermediate situation. This ternary compound is an indirect-gap semiconductor above a crossover composition x_c,[6,7] or a crossover pressure P_c,[8] respectively. The lowest conduction-band minimum is situated at the X point of the Brillouin zone for both situations. This material system thus provides a large density of states for optically excited electrons just as in Si.[6] The transition probability for indirect electron-hole recombination in $Al_xGa_{1-x}As$ close to the crossover point is, however, largely enhanced with respect to Si or Ge. These indirect transitions proceed via virtually assumed states in the Γ minimum, which are nearly resonant to the initial states at the X point.[9] This results in a lifetime of electron-hole pairs in the nanosecond regime,[10] which is rather comparable to the situation in GaAs. We will show that droplet condensation still occurs in indirect-gap $Al_xGa_{1-x}As$. The nucleation dynamics is, however, 2 orders of magnitude faster than in Si as a consequence of alloy disorder.

The possibility of electron-hole droplet formation in the $Al_xGa_{1-x}As$ system was previously addressed by several authors. Cohen *et al.*[11] reported that the density in an optically excited electron-hole plasma did not change significantly with time. Similar results were obtained in picosecond high-excitation experiments by Kalt *et al.*[10] An electron-hole liquid was proposedly observed in $Al_{0.92}Ga_{0.08}As$, i.e., a material close to pure AlAs, by Bimberg *et al.*[12] Again, the interpretation of the luminescence experiments was based mainly on observation of a constant plasma line shape.

The dependence on excitation fluence and the temporal development of the electron-hole system surely can give first hints on the presence of a liquid phase in a highly excited semiconductor. An unambiguous proof of this condensation process is, however, only achieved if a phase diagram of the electron-hole system is determined or the phase separation into an exciton gas and the liquid is demonstrated in the experiments. Neither of these criteria has been fulfilled in the above-mentioned experiments. In the following, we will demonstrate both criteria for the condensation in $Al_xGa_{1-x}As$ close to the crossover point. We will also give a consistent description of all experiments on the electron-hole plasma in this indirect-gap semiconductor alloy.

This paper is organized as follows. After the description of the experimental procedures in Sec. II, we will present some typical results of picosecond luminescence spectroscopy in indirect-gap $Al_xGa_{1-x}As$ (III A). A preliminary phase diagram is constructed using parameters extracted from luminescence line-shape fits (III B). The experimental results are then compared to parameters calculated with a model which employs a simple approximation for many-body effects (III C). Some dynamical aspects of the droplet formation and the phase separation will be discussed in Sec. III D. We will then focus on the dynamics of the band-gap narrowing due to many-body effects (III E) and finally present some properties of the plasma above the critical parameters (III F). The paper will be summarized in Sec. IV.

II. EXPERIMENTAL PROCEDURES

We perform photoluminescence studies on a picosecond time scale. The samples are excited by pulses [5 ps full width at half maximum (FWHM)] from a tunable, synchronously pumped dye laser using Rhodamine 6G as the gain medium. The luminescence signal is spectrally and temporally resolved by a combination of a 0.32 m spectrometer and a streak camera with a two-dimensional readout. The temporal resolution of the system is limited by trigger jitter to about 10 ps.

We study a variety of $Al_xGa_{1-x}As$ samples close to the crossover from a direct-gap to an indirect-gap semiconductor. For one, we use thin layers of indirect-gap $Al_xGa_{1-x}As$ with thicknesses of less than 2 μm. These layers are grown by liquid-phase epitaxy on GaAs substrates. The AlAs mole fraction x is determined from photoluminescence excitation spectroscopy and time-integrated photoluminescence at low excitation. The extracted energetic position of the direct absorption edge at He temperature is compared to a reference sample whose x value is determined by high-resolution x-ray diffraction to be $x=0.42$. The luminescence dynamics shows that this sample is right at the crossover composition.[13] All samples are mounted in a He cryostat and kept at a lattice temperature of 5 K.

We further use a direct-gap $Al_xGa_{1-x}As$ epitaxial layer with $x=0.38$. This sample is placed in a diamond-anvil cell with He or Xe as pressure medium.[14] The direct-to-indirect crossover is now achieved by application of high hydrostatic pressure to the sample. The nominal crossover pressure at 5 K for this sample is $P_c=7.5$ kbar. This procedure provides the possibility to simulate the same constellation of Γ and X minima in the conduction band as in indirect $Al_xGa_{1-x}As$ but at a different level of alloy disorder. The energies of the band gaps can be tuned in this case without changing the sample, i.e., there is no influence of varying sample quality and the alloy disorder remains fixed.

Finally, we used a thin GaAs layer (0.6 μm thick) grown between two 7-μm-thick $Al_{0.30}Ga_{0.70}As$ barrier layers. The GaAs substrate was completely removed to eliminate the luminescence from the substrate. This sample is an indirect-gap semiconductor for hydrostatic pressures in excess of 42 kbar.[8] Again, the same constellation for Γ and X minima is achieved, but now without any influence of alloy disorder.

III. RESULTS AND DISCUSSION

A. Temporal evolution of the luminescence

We first want to discuss in detail the picosecond luminescence studies on the $Al_{0.38}Ga_{0.62}As$ sample under hydrostatic pressure (all experimental data shown in Figs. 1–7 were recorded in this sample). The free and the donor-bound exciton at the X point are the lowest electronic excitations at a hydrostatic pressure of 6.9 kbar for very low excitation.[15] The luminescence of the donor-bound exciton saturates for increasing excitation level and a broad emission due to bimolecular recombination of electron-hole pairs is detected. The electrons of this plasma reside predominantly in the X minima. The recombination processes for free excitons as well as for the plasma proceed without the participation of phonons. This process is a consequence of the relaxation of the momentum conservation by alloy disorder[16] and dominates the recombination in $Al_xGa_{1-x}As$ samples close to the crossover point.[17]

The temporal evolution of the luminescence spectra at an excitation level of $F_{low}=2.2$ $\mu J/cm^2$ is depicted in Fig. 1. The excess energy of the pump laser is about 30 meV. The initial carrier temperature is thus distinctly elevated, but the cooling of the electron-hole system to some 50 K takes only few picoseconds in an indirect-gap semiconductor at low excitation.[18] The luminescence progressively splits up into two lines. The narrow line at higher photon energies coincides with the free exciton at the indirect gap observed in time-averaged luminescence at very low excitation. The luminescence from less-excited areas of the sample was eliminated by imaging the excited spot on the sample onto a pinhole. The exciton luminescence thus originates from the center of the excited spot. The broad line at lower photon energies shows some red shift with time, but is nearly constant in line shape for times longer than 200 ps. We will prove below that this emission stems from the recombination in condensed electron-hole droplets. The series of luminescence spectra in Fig. 1 thus shows the dynamics of the phase separation of an electron-hole plasma into a condensed liquid and an excitonic gas.

B. Experimental phase diagram and critical parameters

An unambiguous proof of droplet condensation is only given when the density in the droplets is shown to decrease with temperature, i.e., when part of the phase diagram can be constructed. In order to give this proof, we extract the experimental plasma parameters from our time-resolved luminescence spectra. We model the line shape $I(\hbar\omega)$ of spectra at long delay times, i.e., when this

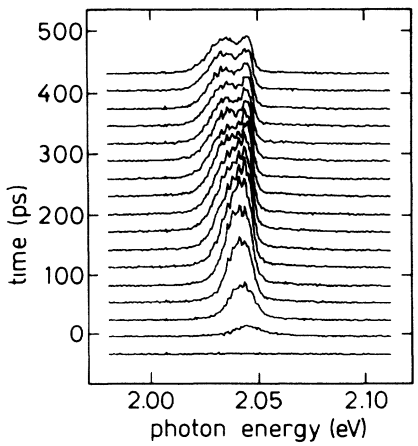

FIG. 1. Temporal development of the luminescence signal in $Al_{0.38}Ga_{0.62}As$ at a hydrostatic pressure of $P=6.9$ kbar and for excitation with 2.2 $\mu J/cm^2$.

line shape is nearly constant in time. The plasma luminescence is fitted by the convolution of the joint density of states and the Fermi functions $f_{e,h}(E,n,T)$ for electrons and holes as is appropriate for indirect transitions.[19]

$$I(\hbar\omega) \propto \int_0^{\hbar\omega - E_g'} E^{1/2}(\hbar\omega - E - E_g')^{1/2} f_e f_h dE \ . \quad (1)$$

The exciton line shape is given by[2]

$$I(\hbar\omega) \propto (\hbar\omega - E_{\mathrm{FE}})^{1/2} \exp\left[-\frac{\hbar\omega - E_{\mathrm{FE}}}{k_B T} \right] . \quad (2)$$

Only zero-phonon recombination is taken into account. Phonon sidebands only play a role for larger separations of Γ and X minima, i.e., for higher pressures or x values, respectively.[17] The fit parameters are the renormalized indirect band gap E_g', the pair density n, the energy of the free exciton E_{FE}, and the common temperature T for the excitons and the plasma.

A typical result of this procedure is shown in Fig. 2. The experimental line shape is well reproduced by our model. Some minor mismatch remains at the low-energy sides of the exciton and plasma line shape. Resonant excitation of the exciton at low fluence shows that part of the tail in the exciton line results from localized excitons. Additional contributions might stem from recombination accompanied by inelastic scattering. No broadening due to final state damping accompanied by plasmon excitation[1,2] is included in the plasma line shape. Especially in the case of indirect recombination, this mechanism is expected to change the fit parameters only slightly.

We find from the line-shape fits that the plasma parameters for long delay times are not directly dependent on the excitation density in the range between 1 and 16 μJ/cm^2. The only consequence of the increased excitation level is that the carrier temperature is slightly higher. The carrier density for $t > 200$ ps is always in the range of $(3-4)\times 10^{18}$ cm^{-3}, although the excitation fluence is varied by a factor of 16. The dependence of the carrier density on the carrier temperature for these conditions is shown in Fig. 3 (crosses). The n-T diagram

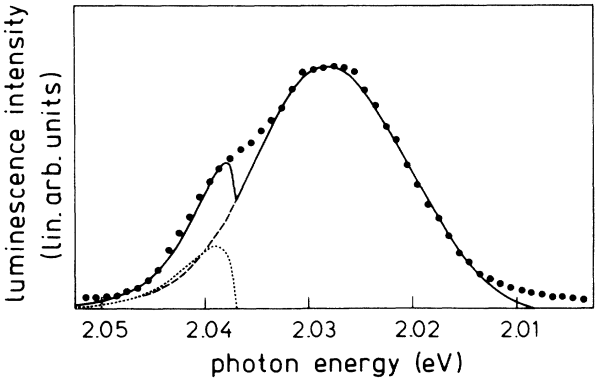

FIG. 2. Fit (solid line) to a photoluminescence spectrum (dots) at a time delay of 360 ps after excitation with 16 μJ/cm^2. Dashed line, electron-hole droplet; dotted line, free exciton. The fit parameters are $n = 4\times 10^{18}$ cm^{-3} and $T = 30$ K.

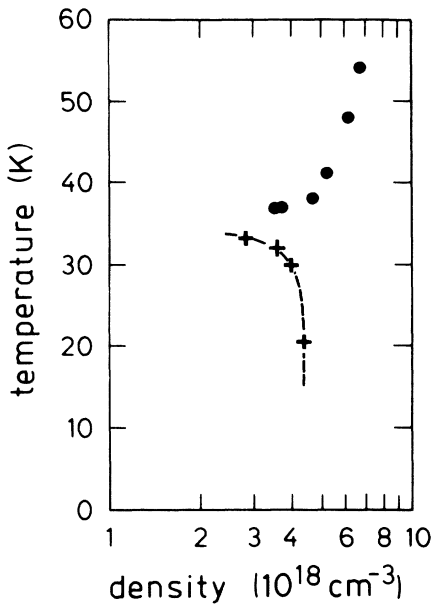

FIG. 3. Temperature-density diagram for $Al_{0.38}Ga_{0.62}As$ ($P = 6.9$ kbar). Dashed line, proposed phase diagram (see text).

shows exactly the signature of an electron-hole-liquid phase diagram, i.e., the density decreases with rising temperature. This is definite proof for the condensation into electron-hole droplets.

A first experimental phase diagram is given by simply connecting the experimental points (dashed line in Fig. 3). It is clear that more data, especially for stationary excitation conditions, are necessary to complete this diagram. It is possible, however, to get reasonable estimates of the liquid parameters. The critical temperature T_c is estimated to be 34 K, the critical density n_c, and the ground-state density n_0 are about 2×10^{18} and 4.5×10^{18} cm^{-3}, respectively (see Table I). The binding energy of the liquid E_{bind}, which is determined by the difference between the chemical potential of the liquid and the energy of the free exciton, is found to be $6(\pm 2)$ meV. These liquid parameters are similar to the ones found in Si.[1]

The plasma density and temperature for the case of excitation with $F_{\max} = 64$ μJ/cm^2 is represented by the dots in Fig. 3. The carrier temperature here stays above T_c for times up to 500 ps. The carrier density increases with temperature for this excitation level. We will discuss the properties of the electron-hole plasma above the critical parameters in more detail in Sec. III F.

C. Theoretical model

We want to describe in this section a simple model to estimate the theoretically expected parameters of the

TABLE I. Electron-hole liquid parameters.

	n_0 (cm^{-3})	E_{bind} (meV)	n_c (cm^{-3})	T_c (K)
theory	3×10^{18}	9.6	1×10^{18}	25
experiment	4.5×10^{18}	$6(\pm 2)$	2×10^{18}	$34(\pm 2)$

electron-hole liquid. Only the band-structure and exciton parameters of the material under investigation are essentially needed in this model. The many-body effects are treated by a simple approximation.

We first determine the equilibrium density n_0 and the binding energy $E_{\rm bind}$ of the liquid phase. We start with a calculation of the ground-state energy E_G at $T=0$ K from[1]

$$E_G=\bar{E}_{\rm kin}+E_{\rm xc} \ . \tag{3}$$

The average kinetic energy $\bar{E}_{\rm kin}$ is determined for a given carrier density n by the Fermi energies $E_F^{e,h}$ of electrons and holes:

$$\bar{E}_{\rm kin}(n)=\tfrac{3}{5}[E_F^e(n)+E_F^h(n)] \ . \tag{4}$$

We use the band parameters[6] of $Al_{0.45}Ga_{0.55}As$ for the calculation of the density-of-states masses needed in Eq. (2). The exchange-correlation energy $E_{\rm xc}$, which describes the self-energy corrections due to many-body effects in the electron-hole system, is approximated in units of the excitonic Rydberg Ry* by the universal formula of Vashishta and Kalia:[20]

$$E_{\rm xc}(r_s)=\frac{a+br_s}{c+dr_s+r_s^2} \ , \tag{5}$$

where a, b, c, and d are universal constants (see Ref. 20) and r_s is the normalized interparticle distance determined by the carrier density and the excitonic Bohr radius a_B:

$$r_s=\left[\frac{3}{4\pi n}\right]^{1/3}\frac{1}{a_B} \ . \tag{6}$$

The minimum of the ground-state energy as a function of r_s defines the ground-state density n_0 and the liquid binding energy $E_{\rm bind}$.

The critical parameters of the liquid phase are determined from a calculation of a set of isotherms of the chemical potential μ as a function of pair density n:

$$\mu(n,T)=E_g'(n)+E_F^e(n,T)+E_F^h(n,T) \ . \tag{7}$$

We again use $E_{\rm xc}$ from the universal formula [Eq. (5)] to calculate the renormalized band gap E_g' in Eq. (7):

$$E_g'=E_g+\Delta E_g=E_g+n\frac{\partial}{\partial n}E_{\rm xc}+E_{\rm xc} \ . \tag{8}$$

It was shown in Ref. 21 that this is valid in indirect-gap $Al_xGa_{1-x}As$. The critical temperature T_c is then given by the isotherm of the chemical potential μ, whose derivative at the turning point is zero. Finally, the critical density n_c is calculated from the scaling law $n_c/n_0=0.34$.[22]

The experimental and calculated parameters are summarized in Table I. The data are in reasonable agreement, although we used a rather crude approximation for the many-body effects. This agreement strongly supports the interpretation of our experimental data in terms of a fast droplet formation.

D. Dynamics of droplet formation and phase separation

The experimental phase diagram of indirect-gap $Al_xGa_{1-x}As$ close to the crossover point is found to be very similar to the one in Si. This is expected considering the similarity of the exciton parameters in both materials. The formation of electron-hole droplets in Si was measured to occur on a time scale of 50 ns.[23] The nucleation dynamics in $Al_xGa_{1-x}As$ is obviously much faster, illustrating some distinct differences between an elemental and an alloy semiconductor.

The onset of the droplet luminescence (Fig. 4) in $Al_xGa_{1-x}As$ depends on the excitation fluence, or the density of initially excited carriers, respectively. The onset time is faster for excitation at $F_{\rm med}$, which corresponds to an initial carrier density $n_{\rm in}$ of 5×10^{17} cm^{-3}, than for $F_{\rm low}$ ($n_{\rm in}=7\times10^{16}$ cm^{-3}). The initial densities are estimated from the absorption coefficient. The luminescence decay, however, is exactly equal for both excitation densities.[24] This demonstrates that stable droplets have formed within about 150 ps.

The rather fast dynamics of the droplet formation indicates that the condensation in indirect-gap $Al_xGa_{1-x}As$ occurs from the plasma phase, in contrast to Si, where first free excitons are formed. The free excitons in Si first cluster to multiexciton complexes and eventually form droplet embryos which grow to macroscopic size.[3] No multiexciton lines, only free-exciton and bimolecular recombination in the liquid, are observed in $Al_xGa_{1-x}As$.

A huge number of tiny droplets thus appears to nucleate in the alloy semiconductor. An equilibrium with the simultaneously forming excitonic gas phase can only be reached once the droplets have grown big enough, i.e., when the droplet surface is large enough for an efficient exchange of excitons through it. Consequently, the droplets are not necessarily in equilibrium with the exciton gas surrounding them. An equilibrium implies a common temperature for excitons and droplets, i.e., a fit to the overall luminescence line shape is possible with a common temperature as described above.

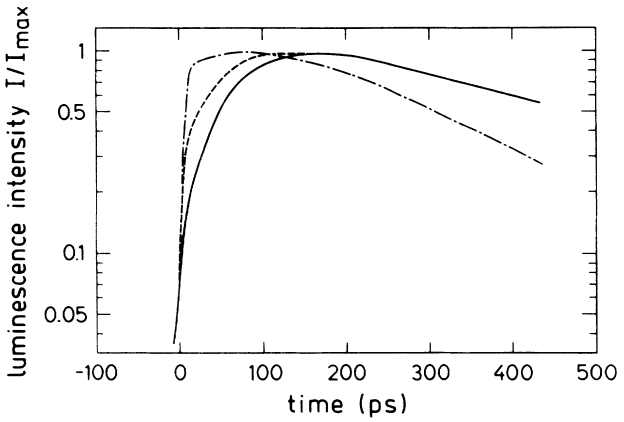

FIG. 4. Time dependence of the spectrally integrated electron-hole luminescence for various excitation levels. Solid line, $F_{\rm low}$; dashed line, $F_{\rm med}$; dashed-dotted line, $F_{\rm max}$.

However, this is not the case for low excitation levels and short delay times after the excitation pulse. Here, it is only possible to fit the line shape of the two entities separately. The temperature of the exciton gas is always found to be lower than the temperature of the liquid. A common temperature for both subsystems is reached at about 200 ps for F_{med} and 360 ps for F_{low}. No equilibrium, however, is reached for even lower excitation at 1 μJ/cm^2 within 1 ns. The achievement of an equilibrium phase separation depends, as expected, on the initially excited carrier density, i.e., on the size of the droplets.

A large number of tiny droplets implies of course that a huge number of condensation seeds is available. These condensation seeds are inherently provided in $Al_xGa_{1-x}As$ by the random potential fluctuations due to alloy disorder.[16,25] We prove this point by studying the nucleation dynamics in different samples. We find that the dynamics of droplet formation is even faster in samples with slightly higher disorder (e.g., about 120 ps in $Al_{0.42}Ga_{0.58}As$). No droplet formation at all, however, is observed in GaAs, which is indirect due to application of hydrostatic pressure. The pair luminescence in the latter case for all excitation levels is consistent with an electron-hole plasma phase, i.e., the density increases with temperature. Of course, no disorder is present in this sample. The velocity of nucleation thus scales with the amount of alloy disorder in the material, which immediately explains the differences between Si and $Al_xGa_{1-x}As$.

E. Band-gap renormalization

Many-body effects in the electron-hole system lead to a strong reduction of the quasiparticle self-energies.[1] One result of this reduction is the narrowing of the band gap in the highly excited semiconductor. This band-gap renormalization is directly accessible in the luminescence experiment, because the band-gap energy determines the low-energy tail of the emission. In the case of the fundamental band gap, both exchange and correlation effects contribute to the narrowing. It was shown in Ref. 21 that the renormalization in indirect-gap $Al_xGa_{1-x}As$ is well described by Eqs. (8) and (5).

The dynamics of the band-gap renormalization ΔE^X_{gap} for the electron-hole system below and above the critical parameters is illustrated in Fig. 5. We observe a renormalization increasing with time in the case of condensation to electron-hole droplets (F_{low} and F_{med}). Two processes can contribute to the band-gap narrowing: first, the carrier density in the droplets increases as a result of carrier cooling by emission of acoustic phonons. Secondly, the average surface energy per carrier decreases when the droplets grow in size.[4]

We want to illustrate the magnitude of both effects for the example of medium excitation. The pair density in the droplets for $t=120$ and 360 ps is 3.86×10^{18} and 4.04×10^{18} cm^{-3}, respectively. The theoretical renormalizations are calculated according to Eq. (8) to be 43 and 44 meV. The experimental values [39($\pm$2) and 42($\pm$2) meV], which are extracted from our line shape fits, are only slightly smaller than theoretically predicted and

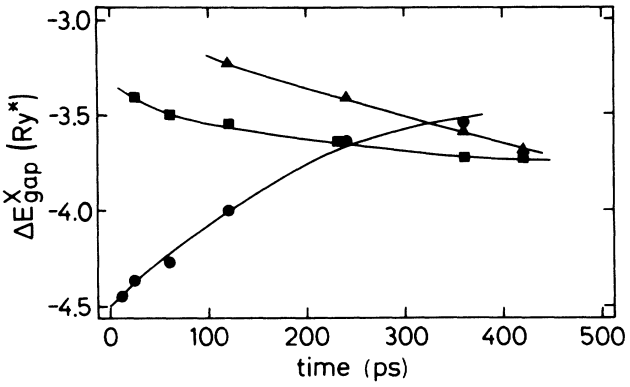

FIG. 5. Temporal development of the renormalization ΔE^X_{gap} of the indirect gap in units of the excitonic Rydberg (11 meV) for various excitation levels. Triangles, F_{low}; squares, F_{med}; dots, F_{max}. The solid lines are guides to the eye.

show the same tendency to increase.

The contribution of the surface energy to the renormalization is calculated from[4]

$$\Delta E_g = \tfrac{2}{3} 4\pi R_N^2 \frac{\sigma}{N} . \tag{9}$$

Here, N is the number of electron-hole pairs in the droplets, σ is the surface tension, and R_N is the radius of the droplets given by

$$R_N = \left[\frac{3}{4\pi} \frac{N}{n_0} \right]^{1/3} . \tag{10}$$

No many-body calculation is, to our knowledge, available for the value of the surface tension in $Al_xGa_{1-x}As$. We thus assume $\sigma = 10^{-2}$ erg/cm^2, which corresponds to the magnitude of the surface tension in Si.[3] This assumption is reasonable, because optical masses and the static dielectric constant are very similar in both materials. The resulting contribution to the renormalization is only significant for rather small droplets, e.g., $\Delta E_g = 2$ meV for $N=6$ and $\Delta E_g = 1$ meV for $N=50$. The droplet dynamics, which was discussed in the previous section, indicates that small droplets are dominant in the materials under consideration.

We conclude from these calculations that both increasing density and reduction of surface energy are of the correct magnitude and can contribute to the experimentally observed temporal shift of the band gap (Fig. 5). The method of luminescence line-shape analysis, however, is limited to an accuracy of about $\pm$2 meV for the determination of the experimental band gap. We are thus not able to explicitly separate both contributions.

The temporal development of the band-gap renormalization for the case of high excitation level shows a completely different behavior than just discussed: the band gap increases with time. The experimental values of the renormalized band gap are in excellent agreement with Eq. (8), which is demonstrated in Fig. 6. We want to dis-

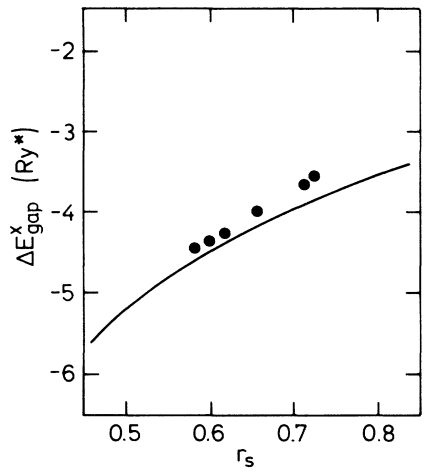

FIG. 6. Band-gap renormalization for excitation with F_{max}. The dots are the experimental values determined from fits to spectra at a various delay times after excitation (compare dots in Fig. 3). The solid line is the theoretical band-gap narrowing according to Eq. (8).

cuss some properties of this electron-hole plasma phase above the critical parameters in the next section.

F. The electron-hole plasma above the critical parameters

We have already proven that the properties of the electron-hole system for excitation with F_{max} correspond to the expected behavior of a plasma phase above the critical parameters. The signatures of this phase are in many respects different from the liquid. Both temperature and density decrease in time (see dots in Fig. 3), which causes a shift of the band gap to higher energies (Figs. 5 and 6).

The determination of the chemical potential of the plasma shows that the plasma phase in indirect-gap $Al_xGa_{1-x}As$ is still bound with respect to the free exciton. The binding energy of the plasma increases in time (see Fig. 7) and approaches the binding energy determined for the liquid phase (6 meV). Consequently, this plasma phase is self-confined, i.e., it does not expand. A phase transition to a liquid state is, however, not possible, because the carrier temperature does not drop below the critical temperature within the rather short lifetime of the electron-hole pairs.

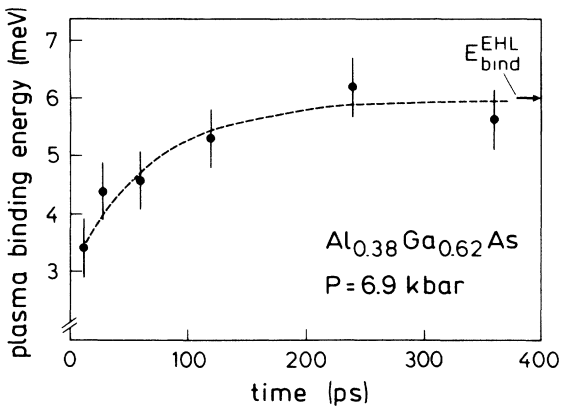

FIG. 7. Binding energy of the plasma phase for excitation with F_{max} as a function of time. The dashed line is a guide to the eye.

That the plasma state is self-confined is supported by comparison to our theoretical model. The band-gap renormalization of an expanding electron-hole plasma is found to deviate significantly from the theoretical behavior [Eq. (5)], unless the line-shape analysis is corrected for the drift velocity of the carriers.[26] Theory and experiment in the case of high excitation in our samples, however, are in excellent agreement without any correction, confirming that a plasma expansion does not occur. The tendency of the plasma to a self-confinement is further proven by a comparison of the plasma density with the initially excited carrier density. The latter one is estimated from the excitation fluence and the absorption coefficient to be 2×10^{18} cm^{-3}. The density in the plasma (see Fig. 3), however, is about a factor of 3 higher. Similar arguments for a confinement of the plasma above T_c were also given by Cohen *et al.*[11] They were, however, not able to determine the critical parameters of the plasma.

A definite distinction between the phases of the electron-hole system in indirect-gap $Al_xGa_{1-x}As$, i.e., between liquid and self-confined plasma, is only possible by their density versus temperature characteristics. The density in the incompressible liquid phase varies only little in time, if at all, and decreases with rising temperature. The density in the confined plasma increases with temperature. Its temporal evolution, however, strongly depends on experimental conditions such as the initially excited pair density. For sufficiently long carrier lifetimes, as can be reached in samples with barrier layers, the plasma density does not vary significantly in time, because the self-confinement counterbalances the carrier losses by recombination. It was shown in Ref. 21 that the band-gap renormalization, even for carrier densities in excess of 10^{19} cm^{-3}, is well described by theory. This is consistent with a negligible expansion of the plasma even for extremely high carrier densities. The plasma, however, is far above the critical parameters for liquid formation as a result of extremely high excitation fluences. These conditions prevailed in the experiments of Cohen *et al.*,[11] Bimberg *et al.*,[12] and Kalt *et al.*[10] Their observations are consistent with the properties of a self-confined plasma phase.

The occurrence of this self-confinement on a picosecond time scale is actually rather surprising. Negative diffusion constants resulting from temperature gradients were proposed by the nonequilibrium thermodiffusion model.[27] Diffusion, however, is not expected to be significant on a picosecond time scale. It thus seems that the properties of the plasma phase in $Al_xGa_{1-x}As$ cannot be explained in the framework of the theories developed for Si and Ge. At this point we can only speculate about the reason for these differences. The nucleation of droplets in Si occurs on a scale that is longer than the time constants for diffusion. This is in

contrast to the results in $Al_xGa_{1-x}As$. Here, the nucleation dynamics, and thus also a possible buildup of local-density fluctuations in the plasma phase, is extremely fast, presumably as a result of the alloy disorder. It is clear that much more theoretical and experimental work is necessary to achieve a comprehensive understanding of these nonequilibrium phenomena.

IV. SUMMARY

The electron-hole system in indirect-gap $Al_xGa_{1-x}As$ undergoes a phase transition to a liquid state on a time scale of a few hundred picoseconds. The velocity of this phase transition scales with the amount of alloy disorder in the material and is orders of magnitude faster than in elemental indirect-gap semiconductors. The achievement of a thermal equilibrium of the electron-hole droplets with the surrounding gas of free excitons depends on the density of initially excited carriers. We are able to construct a first experimental phase diagram and estimate the critical parameters and the ground-state density of the liquid phase. The many-body effects in the plasma, especially band-gap renormalization, can be described consistently by a simple theoretical model. The electron-hole plasma above the critical parameters is still bound with respect to the free exciton and is thus self-confined. Previous experimental observations in indirect-gap $Al_xGa_{1-x}As$ published by other authors can be explained consistently when this self-confinement is taken into account.

ACKNOWLEDGMENTS

We want to acknowledge the expert technical assistance by K. Rother and H. Klann, valuable discussions with G. Mahler, and a critical reading of the manuscript by R. Cingolani. We thank J. Nagle for performing the high-resolution x-ray diffraction, and I. Silier for the preparation of the GaAs sample.

[1]T. M. Rice, in *Solid State Physics,* Vol. 32, edited by H. Ehrenreich, F. Seitz, and D. Turnbull (Academic, New York, 1977), p. 1.

[2]J. C. Hensel, T. G. Phillips, and G. A. Thomas, in Ref. 1, p. 88.

[3]R. M. Westervelt, in *Electron-Hole Droplets in Semiconductors,* edited by C. D. Jeffries and L. V. Keldysh (North-Holland, Amsterdam, 1983), p. 187 and references therein.

[4]H. Haug and F. F. Abraham, Phys. Rev. B **23**, 2960 (1981).

[5]K. Bohnert, M. Anselment, G. Kobbe, C. Klingshirn, H. Haug, S. W. Koch, S. Schmitt-Rink, and F. F. Abraham, Z. Phys. B **42**, 1 (1981).

[6]H. C. Casey and M. B. Panish, *Heterostructure Lasers Part A* (Academic, New York, 1978).

[7]D. J. Wolford, W. Y. Hsu, J. D. Dow, and B. G. Streetman, J. Lumin. **18/19**, 863 (1978).

[8]D. J. Wolford and J. A. Bradley, Solid State Commun. **53**, 1069 (1985).

[9]H. Kalt, A. L. Smirl, and T. F. Boggess, J. Appl. Phys. **65**, 294 (1989).

[10]H. Kalt, K. Bohnert, D. P. Norwood, T. F. Boggess, A. L. Smirl, and I. J. D'Haenens, J. Appl. Phys. **62**, 4187 (1987).

[11]E. Cohen, M. D. Sturge, M. A. Olmstead, and R. A. Logan, Phys. Rev. B **22**, 771 (1980).

[12]D. Bimberg, W. Bludau, R. Linnebach, and E. Bauser, Solid State Commun. **37**, 987 (1981).

[13]There are several conflicting reports on the actual value of the crossover composition and the exact dependence of the band-gap energies E_g on x. Our measurements on the liquid formation do not depend on an absolute determination of the x values of our samples. The gap nature of our samples follows directly from their luminescence characteristics and is not deduced from any of the available $E_g(x)$ calibrations. The accuracy of the determination of relative x values by x-ray diffraction is rather good (± 0.002). Concerning the absolute value of the AlAs mole fraction, our data are in reasonable agreement with the low-temperature measurements of Ref.7.

[14]A. Jayaraman, Rev. Mod. Phys. **55**, 65 (1983).

[15]Our sample shows at 6.9 kbar the following interesting scenario: the lowest conduction-band minimum is located at the Γ point; the lowest electronic excitations, however, are the free and bound exciton at the X point. This can be deduced from time-resolved spectroscopy at very low excitation. The lowest minimum in the case of high excitation is the X minimum due to the different renormalization of minima with different population. Details of these studies will be published elsewhere. Compare also H. Kalt and W. W. Rühle, in *Conference on Quantum Electronics and Laser Science Technical Digest Series* (Optical Society of America, Washington, D.C., 1989), Vol. 12, p. 126.

[16]A. N. Pikhtin, Fiz. Teck. Poluprovodn. **11**, 425 (1977) [Sov. Phys.—Semicond. **11**, 245 (1977)].

[17]H. Kalt, K. Reimann, W. W. Rühle, K. Syassen, and E. Bauser, Ref. 15, p. 51.

[18]W. W. Rühle, K. Leo, and E. Bauser, Phys. Rev. B **40**, 1756 (1989).

[19]G. Lasher and F. Stern, Phys. Rev. **133**, A553 (1964).

[20]P. Vashishta and R. K. Kalia, Phys. Rev. B **25**, 6492 (1982).

[21]K. Bohnert, H. Kalt, A. L. Smirl, D. P. Norwood, T. F. Boggess, and I. J. D'Haenens, Phys. Rev. Lett. **60**, 37 (1988); H. Kalt, K. Bohnert, A. L. Smirl, and T. F. Boggess, in *Proceedings of the Nineteenth International Conference on the Physics of Semiconductors,* edited by W. Zawadski and J. M. Langer (Polish Academy of Science, Warsaw, 1988), p. 1377.

[22]A. Forchel, B. Laurich, J. Wagner, W. Schmid, and T. L. Reinecke, Phys. Rev. B **25**, 2730 (1982).

[23]J. Collet, J. Barreau, M. Brousseau, and H. Maaref, Phys. Status Solidi B **80**, 461 (1977).

[24]The luminescence decay time for the electron-hole droplets in this sample is 410 ps. This time appears to some extent to be sensitive to the sample quality and design. We find decay times of several nanoseconds in samples with optimized growth conditions and barrier layers between substrate and active layer. These decay times are, however, of the same time scale as the repetition rate of the pump laser. A time-resolved study of the droplet dynamics is then not possible.

[25]F. Oosaka, T. Sugano, Y. Okabe, and Y. Okada, Jpn. J. Appl. Phys. **15**, 2371 (1976).

[26]A. Forchel, H. Schweizer, and G. Mahler, Phys. Rev. Lett. **51**, 501 (1983).

[27]G. Mahler, G. Maier, A. Forchel, B. Laurich, H. Sanwald, and W. Schmid, Phys. Rev. Lett. **47**, 1855 (1981).